Temperature dependence of the bulk Rashba splitting in the bismuth tellurohalides

Bartomeu Monserrat[1,2,*] and David Vanderbilt[1]

[1]*Department of Physics and Astronomy, Rutgers University, Piscataway, New Jersey 08854-8019, USA*

[2]*TCM Group, Cavendish Laboratory, University of Cambridge, J. J. Thomson Avenue, Cambridge CB3 0HE, United Kingdom*

We study the temperature dependence of the Rashba-split bands in the bismuth tellurohalides BiTeX ($X =$ I, Br, Cl) from first principles. We find that increasing temperature reduces the Rashba splitting, with the largest effect observed in BiTeI with a reduction of the Rashba parameter of 40% when temperature increases from 0 to 300 K. These results highlight the inadequacy of previous interpretations of the observed Rashba splitting in terms of static-lattice calculations alone. Notably, we find the opposite trend, a strengthening of the Rashba splitting with rising temperature, in the pressure-stabilized topological-insulator phase of BiTeI. We propose that the opposite trends with temperature on either side of the topological phase transition could be an experimental signature for identifying it. The predicted temperature dependence is consistent with optical conductivity measurements, and should also be observable using photoemission spectroscopy, which could provide further insights into the nature of spin splitting and topology in the bismuth tellurohalides.

I. INTRODUCTION

The spin-orbit interaction, which arises in the nonrelativistic limit of the Dirac equation, is an interaction between the spin and orbital degrees of freedom of electrons in solids that drives a number of phenomena, such as the spin splitting of bands [1] and the band inversion in topological insulators [2,3].

In systems that break inversion symmetry and have a symmetry axis along $\mathbf{e}_3$, the spin-orbit interaction can be characterized by the two-band Rashba Hamiltonian [1,4,5]

$$H_R = \alpha_R \boldsymbol{\sigma} \cdot \mathbf{k} \times \boldsymbol{e}_3, \qquad (1)$$

where α_R is the Rashba parameter which captures the strength of the spin-orbit interaction, $\boldsymbol{\sigma} = (\sigma_1, \sigma_2, \sigma_3)$ are the Pauli matrices, and $\mathbf{k}$ is the three-dimensional crystal momentum. The Rashba Hamiltonian leads to a spin splitting of the electron bands near the band minimum and in the plane perpendicular to $\mathbf{e}_3$, characterized by the Rashba momentum k_R and Rashba energy E_R by which bands of opposite spin polarization are shifted, as shown later in Fig. 2. In terms of these parameters, $\alpha_R = 2E_R/k_R$.

The spin splitting in energy and momentum provided by the Rashba spin-orbit interaction drives a number of interesting phenomena, such as the spin Hall effect [6], the Edelstein effect [7], the spin galvanic effect [8], and superconductivity with noncentrosymmetric pairing [9]. This rich phenomenology can be exploited in spintronic devices, in which external electric and magnetic fields, as well as light, are used to control the spin degrees of freedom [10]. Due to this fundamental and applied interest, a significant research effort is dedicated to the discovery and characterization of materials exhibiting strong Rashba splitting. Rashba splittings have been measured at surfaces [11], interfaces [12], and most recently a giant Rashba effect has been discovered in the bulk and surfaces of the polar bismuth tellurohalides BiTeX ($X =$ I, Br, Cl) [13–16]. We direct the readers to a recent review that highlights the

quantum phenomena associated with the spin-orbit physics of the bismuth tellurohalides [17].

First-principles methods have been used to interpret experimental measurements of the Rashba splitting in the bismuth tellurohalides and to understand the microscopic origin of the effect [13–19]. With this understanding, it becomes possible to use first-principles calculations to search for other materials exhibiting large bulk Rashba effects, an effort that has led to the proposal and discovery of a number of promising candidates [20–23]. Most first-principles calculations in this context are based on semilocal approximations to density functional theory (DFT), although some recent work has highlighted that van der Waals dispersion corrections [24] and many-body electron correlations [25] can have large effects on the calculated Rashba parameters. These calculations are invariably performed within the static lattice approximation, which for materials containing heavy elements with small quantum zero-point energies is approximately equivalent to zero temperature. This could make comparison with experiment problematic, as measurements are typically performed at finite temperatures. Furthermore, as the effects of temperature on Rashba splitting are at present poorly known, this also raises the question of the relevance of first-principles predictions of novel Rashba materials for spintronic applications, as devices would be required to operate at room temperature.

In this work we use first-principles methods to study the role of temperature on the Rashba-split electronic states. The temperature dependence of electronic states has two origins: electron-phonon coupling and thermal expansion. We explore both contributions to the bulk Rashba splitting of the bismuth tellurohalides, and find that their contributions are comparable. We find that the Rashba parameter decreases with increasing temperature, with the strongest change observed in BiTeI for which α_R decreases by 40% in the conduction bands from 0 to 300 K. We also predict the opposite trend, an enhancement of Rashba splitting with increasing temperature, in the topological-insulator phase of BiTeI, which is stabilized under hydrostatic pressure. This result suggests that monitoring the sign of the band gap change with temperature could be a useful signature for identifying a topological phase transition.
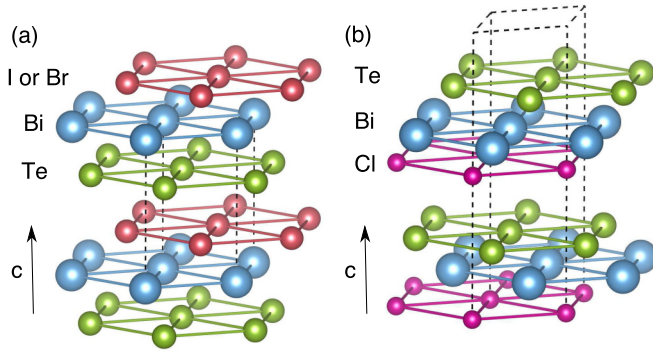
*bm418@cam.ac.uk

FIG. 1. Structures of (a) BiTeI and BiTeBr, and (b) BiTeCl. The layers are stacked along the c direction, and the stacking leads to a trigonal $P3m1$ space group in BiTeI and BiTeBr, and to a hexagonal $P6_3mc$ space group with doubled cell in BiTeCl. The primitive cells are indicated with dashed lines.

Our results imply that quantitative first-principles predictions of Rashba splitting cannot neglect the effects of temperature.

The rest of the paper is organized as follows. In Sec. II we describe the theoretical formalism used for the description of temperature, and provide the computational details of the first-principles calculations. We present the temperature dependence of the Rashba splitting of the bulk bismuth tellurohalides in Sec. III A. In Sec. III B we describe our results for BiTeI in the topological-insulator phase. We discuss the consequences of our results for theory and experiment in Sec. III C, and summarize our findings in Sec. IV.

II. COMPUTATIONAL DETAILS

A. First-principles calculations

We perform first-principles calculations based on DFT using VASP [26–29] and the projector augmented-wave method [30,31]. We choose an energy cutoff of 500 eV and a **k**-point grid of size $8 \times 8 \times 8$ for BiTeI and BiTeBr, and $8 \times 8 \times 4$ for BiTeCl. For the supercell calculations we use commensurate grids. All calculations are performed including the spin-orbit interaction with the second variational method [32], in which the spin-orbit interaction is included as a perturbation to the scalar relativistic Hamiltonian.

B. Structural properties

The bismuth tellurohalides are layered materials with a polar structure as shown in Fig. 1. The structure of BiTeI belongs to the trigonal $P3m1$ space group, where the stacking direction c is also the polar axis [33]. Early x-ray powder

diffraction data for BiTeBr revealed a structure similar to that of BiTeI, but with random disorder in the Te and Br sites [33]. A more recent study reports an ordered phase of the same symmetry as BiTeI replacing the I atoms by Br atoms [16], and in this work we use the latter ordered phase. The structure of BiTeCl is also ordered, but the stacking differs from that of BiTeI; the primitive cell is doubled along the stacking direction, resulting in a structure in the hexagonal space group $P6_3mc$ [33].

DFT calculations are performed to relax the lattice parameters and internal coordinates with residual forces below 1 meV/Å and residual stresses below 0.01 GPa. The relaxed lattice parameters are provided in Table I, and the results have been obtained using the local density approximation (LDA) to the exchange correlation functional [34–36], the generalized gradient approximation of Perdew-Burke-Ernzerhof (PBE) [37], the PBE approximation for solids (PBEsol) [38], and the PBE approximation with the Tkatchenko-Scheffler van der Waals correction (PBE+TS) [39]. A comparison with the reported experimental lattice parameters from Ref. [33] suggests that the cell volumes are most accurately captured by the PBEsol functional.

The only free internal parameters are the distances between the Bi-Te and Bi-halide planes, which we show in Table II for the same selection of exchange-correlation functionals. For BiTeI, it has previously been pointed out [18] that the experimental assignment had the Te and I locations reversed, an error attributed to the similar x-ray scattering strengths of Te and I. Taking this into account, the structures obtained using the semilocal functionals are in good agreement with the experimental structure. For BiTeBr, the reported structure is such that the Te and Br sites exhibit random disorder, and therefore there is a unique interplanar distance. This distance is intermediate between the calculated interplanar distances for the ordered structure that we use. For BiTeCl, again there is reasonable agreement between theory and experiment.

Overall, the structural study suggests that PBEsol accurately describes the bismuth tellurohalides and we have therefore used this functional for all subsequent calculations. We also note that our calculated structural parameters are in good agreement with previous computational reports [18,40].

C. Electronic properties

The bismuth tellurohalides are small band gap semiconductors exhibiting strong Rashba splitting in both the valence and conduction bands near the band gap minimum. This occurs around the A point at the center of the electronic Brillouin zone on the $k_z = \pi/c$ plane for BiTeI and BiTeBr, and around the Γ

TABLE I. Equilibrium lattice parameters (in Å) of the bismuth tellurohalides using the LDA, PBE, PBEsol, and PBE+TS exchange correlation functionals, and corresponding experimental data from Ref. [33].

	LDA		PBE		PBEsol		PBE + TS		Experiment	
	a	c	a	c	a	c	a	c	a	c
BiTeI	4.31	6.64	4.43	7.46	4.34	6.81	4.33	6.63	4.34	6.85
BiTeBr	4.24	6.28	4.36	7.06	4.27	6.48	4.43	6.74	4.27	6.49
BiTeCl	4.22	11.99	4.32	13.61	4.24	12.50	4.31	12.87	4.24	12.40

TABLE II. Equilibrium distances (in Å) between the Bi-Te and Bi-halide planes in the bismuth tellurohalides using the LDA, PBE, PBEsol, and PBE+TS exchange-correlation functionals, and corresponding experimental data from Ref. [33].

	LDA		PBE		PBEsol		PBE + TS		Experiment	
	Bi-Te	Bi-halide	Bi-Te	Bi-halide	Bi-Te	Bi-halide	Bi-Te	Bi-halide	Bi-Te	Bi-halide
BiTeI	1.71	2.11	1.71	2.11	1.72	2.11	1.78	2.19	2.10	1.72
BiTeBr	1.74	1.88	1.74	1.88	1.75	1.88	1.74	1.87	1.81	1.81
BiTeCl	1.75	1.66	1.76	1.68	1.76	1.68	1.75	1.67	1.76	1.76

point in BiTeCl due to band folding arising from the doubling of the primitive cell along the stacking direction c. The valence band maximum is dominated by Te and halide states of p_z character, whereas the conduction band minimum is dominated by Bi states also of p_z character. Experimental samples exhibit n doping, which makes the Rashba splitting on the conduction bands the most relevant for potential applications.

D. Lattice dynamics

The effects of temperature on the band structure can be divided into contributions from electron-phonon coupling and from thermal expansion. As a starting point to calculate both contributions from first principles, lattice dynamics calculations have to be performed. We use the finite displacement approach [41] to lattice dynamics in conjunction with nondiagonal supercells [42]. For BiTeI we find that vibrational energies calculated from the Fourier interpolation over fine grids starting with coarse grids of sizes $4 \times 4 \times 4$ and $6 \times 6 \times 6$ **q** points are very similar. We therefore report results using a coarse $4 \times 4 \times 4$ **q**-point grid for BiTeI and BiTeBr, and a coarse $4 \times 4 \times 2$ **q**-point grid for BiTeCl. All calculations include the spin-orbit interaction, which has been found to affect the vibrational frequencies of the bismuth tellurohalides significantly [43].

E. Electron-phonon coupling

The electron-phonon coupling contribution to the temperature dependence of an electronic eigenvalue $\epsilon_{n\mathbf{k}}$, labeled by quantum numbers $(n,\mathbf{k})$, is determined within the adiabatic approximation by its expectation value with respect to the vibrational density

$$\epsilon_{n\mathbf{k}}(T) = \frac{1}{\mathcal{Z}} \sum_{\mathbf{s}} \langle \Phi_{\mathbf{s}}(\mathbf{u}) | \epsilon_{n\mathbf{k}}(\mathbf{u}) | \Phi_{\mathbf{s}}(\mathbf{u}) \rangle e^{-E_{\mathbf{s}}/k_{\mathrm{B}}T}. \quad (2)$$

In this equation, the vibrational wave function $|\Phi_{\mathbf{s}}(\mathbf{u})\rangle$ in state $\mathbf{s}$ has energy $E_{\mathbf{s}}$ and is described within the harmonic approximation, $\mathbf{u} = \{u_{\nu\mathbf{q}}\}$ is a collective coordinate for all the nuclei written in terms of normal modes of vibration $(\nu,\mathbf{q})$, $\mathcal{Z} = \sum_{\mathbf{s}} e^{-E_{\mathbf{s}}/k_{\mathrm{B}}T}$ is the partition function, T is the temperature, and k_{B} is Boltzmann's constant.

We evaluate Eq. (2) using a quadratic approximation to $\epsilon_{n\mathbf{k}}(\mathbf{u})$ in terms of normal coordinates [44–47], as well as using a Monte Carlo integration technique [48,49]. The second order expansion coefficients appearing in the quadratic approximation for polar modes diverge in the limit $\mathbf{q} \to 0$ [47], but in practice we find that by choosing a fixed amplitude of $0.5\sqrt{\langle u_{\nu\mathbf{q}}^2 \rangle}$ in a finite differences context leads to good

agreement with the Monte Carlo method, which does not exhibit any divergent behavior. Furthermore, the agreement between the Monte Carlo and quadratic calculations also indicates that multiphonon terms, correctly included in the former, are negligible in these systems. Because nondiagonal supercells can be used in conjunction with the quadratic approximation to efficiently sample the vibrational Brillouin zone [42], we choose this method for the electron-phonon coupling calculations reported below. We also find that the results do not change significantly between grid sizes of $4 \times 4 \times 4$ and $6 \times 6 \times 6$ in BiTeI. We therefore use $4 \times 4 \times 4$ grids for BiTeI and BiTeBr, and $4 \times 4 \times 2$ grids for BiTeCl.

F. Thermal expansion

We evaluate the effects of thermal expansion within the quasiharmonic approximation [50]. We calculate the vibrational free energy at temperature T as a function of the lattice parameters a and c, and minimize the total Gibbs free energy at each temperature with respect to the value of the lattice parameters to determine the equilibrium volume at that temperature. Due to the layered nature of the bismuth tellurohalides, the thermal expansion along the stacking c direction is about an order of magnitude stronger than that along the in-plane direction, and therefore we minimize the Gibbs free energy independently for each lattice parameter to reduce the number of calculations required.

III. TEMPERATURE DEPENDENCE OF THE RASHBA SPLITTING

A. Temperature dependent Rashba splitting in BiTeI, BiTeBr, and BiTeCl

The temperature dependence of the Rashba-split conduction and valence bands of BiTeI, BiTeBr, and BiTeCl is shown in Fig. 2. The contributions from electron-phonon coupling and thermal expansion are plotted separately, showing that their effect is similar in magnitude. The combination of both effects leads to the overall temperature dependence. The bands are referenced with respect to the lowest conduction-band state at the A point in BiTeI and BiTeBr, and to the lowest conduction-band state at the Γ point in BiTeCl. The **k**-space region shown in Fig. 2 only covers about 10% of the Brillouin-zone dimensions.

In all materials, the band dispersion deviates significantly from that of the two-band model of Eq. (1). In particular, we observe an anisotropic Rashba splitting that reflects the hexagonal symmetry of the underlying crystal structure. Nonetheless, it is still common practice to extract Rashba
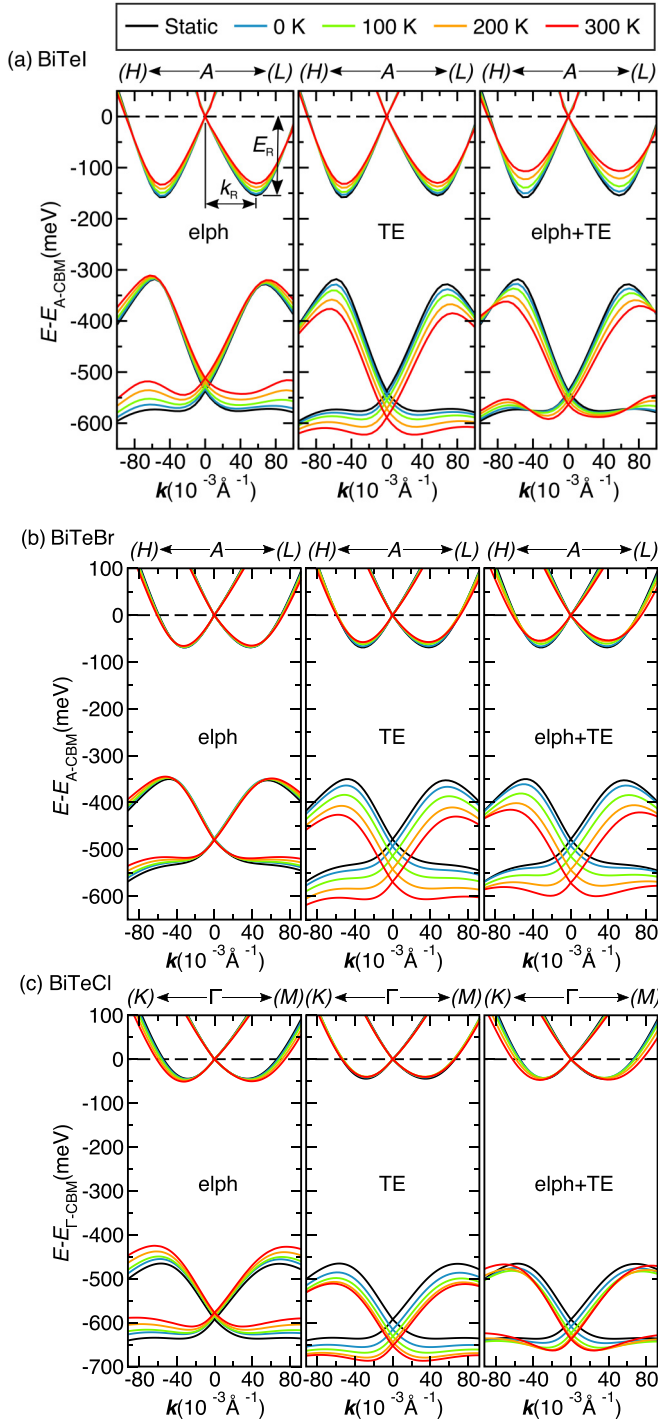
FIG. 2. Temperature dependence of the Rashba-split bands of (a) BiTeI, (b) BiTeBr, and (c) BiTeCl. Contributions from electron-phonon coupling (elph) and thermal-expansion (TE) are combined to obtain the overall temperature dependence (elph+TE) in the left, middle, and right panels, respectively. The electronic states are referenced to the conduction-band minimum at the A point for BiTeI and BiTeBr and the Γ point for BiTeCl. Note that the plotted regions only represent about 10% of the distance from the A or Γ points to the indicated zone boundaries. The definitions of E_R and k_R are depicted in the upper-left panel.
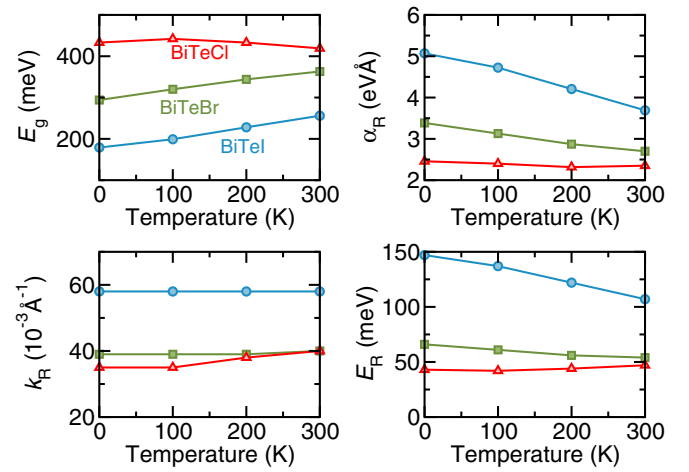

FIG. 3. Temperature dependence of the minimum band gap and of the conduction-band Rashba parameters of the bismuth tellurohalides.

parameters from these band structures, and in the following we will determine k_R and E_R from the dispersion along the A-L line for BiTeI and BiTeBr, and along the Γ-M line for BiTeCl, as indicated in Fig. 2 for BiTeI. We show a summary of the temperature dependence of the minimum band gap and of the Rashba parameters in Fig. 3.

For BiTeI, the E_R parameter of the conduction bands decreases with increasing temperature due to both electron-phonon coupling and thermal expansion. In contrast, the k_R parameter is nearly temperature independent. The E_R parameter of the valence bands shows a weak temperature dependence, while both electron-phonon coupling and thermal expansion lead to an increase in the k_R parameter with increasing temperature. The minimum band gap size increases with increasing temperature. The Rashba parameter of the conduction bands at 0 K of $\alpha_R = 5.07$ eV Å is somewhat smaller than the static lattice parameter value of $\alpha_R = 5.35$ eV Å, a consequence of quantum zero-point motion. With increasing temperature, the Rashba parameter decreases to $\alpha_R = 3.69$ eV Å at 300 K.

For BiTeBr, both electron-phonon coupling and thermal-expansion contributions exhibit the same trends as in BiTeI. However, the electron-phonon coupling contribution is significantly weaker, such that the overall temperature dependence of the Rashba-split bands is dominated by thermal expansion. As in BiTeI, the minimum band gap size increases with increasing temperature, and the Rashba parameter of the conduction bands decreases with increasing temperature. The static Rashba parameter of $\alpha_R = 3.63$ eV Å decreases to $\alpha_R = 3.39$ eV Å at 0 K due to quantum zero-point motion, and to $\alpha_R = 2.70$ eV Å at 300 K due to thermal motion.

For BiTeCl, the electron-phonon contribution is opposite to that calculated in BiTeI and BiTeBr, and with increasing temperature it leads to a reduction of the minimum band gap size and to an increase of the strength of Rashba splitting of the conduction bands. The distinct effects of electron-phonon coupling can be attributed to the larger band gap of BiTeCl compared to that of the heavier bismuth tellurohalides,

which suppresses the interband transitions in favor of the intraband transitions compared to the compounds with smaller band gap [51]. The thermal-expansion contribution in BiTeCl exhibits the same trend as that of BiTeI and BiTeBr, but the temperature dependence is weaker. Overall, the minimum band gap of BiTeCl has a weak temperature dependence, and the Rashba parameter of the conduction band decreases by about 0.01 eV Å from 0 to 300 K, determined by a small increase of the Rashba energy which is overcompensated by a small increase of the Rashba momentum.

We next discuss the origin of the decrease in Rashba splitting with increasing temperature predicted in the bismuth tellurohalides, and we focus on BiTeI which exhibits the strongest changes. Following Bahramy and co-workers, the spin-orbit interaction driving Rashba splitting can be treated within perturbation theory in a $\mathbf{k} \cdot \mathbf{p}$ model, with a leading-order correction to an electronic state $\epsilon_{n\mathbf{k}}$ given by [18]

$$\Delta\epsilon_{n\mathbf{k}} = \sum_{m \neq n} \frac{\langle m\mathbf{k}_0|H_{\mathrm{SOC}}|n\mathbf{k}_0\rangle\langle n\mathbf{k}_0|\Delta\mathbf{k}\cdot\mathbf{p}|m\mathbf{k}_0\rangle}{\epsilon_{n\mathbf{k}_0} - \epsilon_{m\mathbf{k}_0}} + \mathrm{H.c.},$$

(3)

where $\Delta\mathbf{k} = \mathbf{k} - \mathbf{k}_0$ is the crystal momentum measured from a reference $\mathbf{k}_0$ taken to be the A point, $\mathbf{p}$ is the linear momentum, and H_{SOC} is the spin-orbit Hamiltonian. Equation (3) allows us to distinguish three contributions to the strength of Rashba splitting [18]: (i) the magnitude of spin-orbit coupling encoded by H_{SOC}, (ii) the selection rules on the matrix elements in the numerator, and (iii) the energy difference in the denominator. Contribution (i) is well optimized in the bismuth tellurohalides as they are comprised of heavy elements exhibiting strong spin-orbit coupling. Contribution (ii) is also optimal, as the crystal-field splittings of the valence and conduction p bands are of opposite sign, resulting in both valence and conduction band extrema of p_z character. This makes the two bands symmetry equivalent and therefore allows the relevant matrix elements to be nonzero. Bahramy and co-workers argued that contribution (iii) is also optimal in the bismuth tellurohalides, as the small A-point band gaps (Γ point for BiTeCl) make the denominators in Eq. (3) small, enhancing the Rashba splitting [18].

In our analysis, the energy denominator in Eq. (3) becomes temperature dependent and therefore dominates the temperature dependence of the Rashba splitting. We note that the electronic wave functions are also temperature dependent, but we neglect this effect in the following discussion. Thermal expansion increases the interatomic distances and drives the system towards the atomic limit. This leads to an increase in the A-point band gap which therefore reduces the Rashba splitting according to Eq. (3), and in agreement with our first-principles calculations. The electron-phonon contribution is harder to interpret (see first column of Fig. 2): different phonon modes couple differently to electronic states, and although the band gap at the A point decreases with increasing temperature, the minimum band gap increases with increasing temperature. The Bi p_z-like states dominating the conduction band and the Te and I p_z-like states dominating the valence band are oriented along the stacking c direction in the bismuth tellurohalides (see Fig. 1). As a consequence, the phonon modes that dominate electron-phonon coupling are those that correspond to atomic vibrations that change the interlayer distance.

B. BiTeI in the topological-insulator phase

Our results indicate that the Rashba splitting decreases with increasing temperature in the bismuth tellurohalides, driven by both electron-phonon coupling and thermal expansion. The thermal-expansion contribution is determined by the approach to the atomic limit and the associated band-gap increase, as discussed in the previous section. This raises the possibility that in systems with inverted bands, the Rashba splitting would increase with increasing temperature. It has been theoretically predicted that BiTeI undergoes a band inversion and becomes a topological insulator under hydrostatic pressure [52], with the topological phase transition mediated by a Weyl semimetal phase [53,54]. Experimental efforts to confirm this prediction have so far reached contradictory conclusions, with a topological phase transition reported around 2–4 GPa in Refs. [55–59] and no topological phase transition reported in Ref. [60]. Similar discussions exist for BiTeBr and BiTeCl [61–64]. In our calculations we observe a band gap inversion in BiTeI between 1–2 GPa. To establish the topological nature of BiTeI under pressure, we calculate the $Z_2 = (\nu_0; \nu_1\nu_2\nu_3)$ invariant, where ν_0 is the strong topological index and determines whether the material is a strong topological insulator, and $(\nu_1\nu_2\nu_3)$ are the weak topological indices that determine the reciprocal space planes in which band inversions occur. We use the Z2PACK code [65] to calculate Z_2, and follow the adiabatic pumping of Wannier charge centers over the electronic Brillouin zone [66], an approach that is appropriate for systems without inversion symmetry. The resulting Z_2 index is $(1; 001)$, confirming the results of Ref. [52].

Our results at 4 GPa in the topological phase are presented in Fig. 4, where again we show the temperature dependence of the Rashba-split bands near the A point of the electronic Brillouin
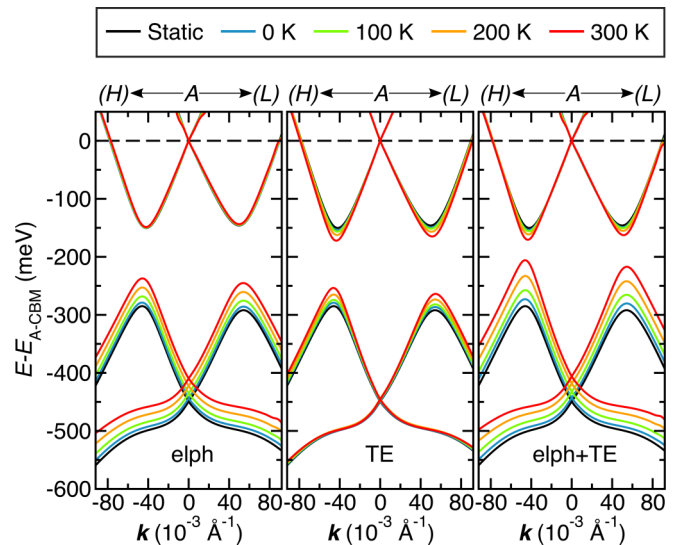

FIG. 4. Temperature dependence of the Rashba-split bands of BiTeI in the topological-insulator phase at 4 GPa. Contributions from electron-phonon coupling (elph) and thermal expansion (TE) are combined to obtain the overall temperature dependence (elph + TE) in the left, middle, and right panels, respectively. The electronic states are referenced to the conduction-band minimum at the A point. We note that the plotted regions only represent about 10% of the distance from the A point to the indicated zone boundaries.

zone. Electron-phonon coupling provides an almost rigid shift of the Rashba-split bands, which leads to a decrease of the minimum and A-point band gaps with increasing temperature. As in the normal phase, the electron-phonon contribution is complex and depends on multiple phonon modes, which overall lead to a small change in the Rashba parameters. As expected, thermal expansion leads to a reduction of the band gap and to an increase of the Rashba splitting with increasing temperature. Overall, the Rashba splitting increases with increasing temperature for both the conduction and valence bands.

In view of these results, we propose a new signature for identifying the topological phase transition in BiTeI. A measurement of the temperature dependence of the minimum band gap or the A-point band gap should show an increase of the band-gap size at pressures in which BiTeI is a normal insulator, and to a decrease of the band-gap size at pressure in which BiTeI is a topological insulator. Monitoring the temperature dependence of the band gap could be a general approach for identifying pressure-induced topological phase transitions [67].

We also note that the temperature dependent spin-split bands shown in Fig. 4 deviate significantly from the canonical dispersion that arises from the Rashba Hamiltonian in Eq. (1). At the topological phase transition, the bands cross linearly in a conelike fashion. In the regime shown in Fig. 4, which is close to the topological phase transition, the bands can be described by two conelike structures which exhibit avoided crossings and therefore deviate significantly from a picture of parabolic intersecting Rashba bands. This effect has been previously described in Ref. [52].

C. Discussion

There are several limitations to our analysis. The first is the description of the electronic degrees of freedom within semilocal DFT. Many-body electron correlations modify the band-gap size and the Rashba splitting strength of the bismuth tellurohalides [25], and a full treatment would require the simultaneous inclusion of electron correlations and temperature. Nonetheless, we expect that the general trends presented in this work would remain [68,69]. The second limitation concerns the neglect of nonadiabatic contributions, which are typically small but could become larger when the band gaps become small. Overall, due to the band-gap underestimation we obtain using semilocal DFT, we expect that our results represent an upper bound on the real temperature dependence of the Rashba splitting of the bismuth tellurohalides. Nonetheless, the temperature dependence that we predict should still be observable experimentally, and we suggest that tuning the band gap to smaller sizes, for example by application of hydrostatic pressure, could enhance the temperature dependence of the Rashba splitting and facilitate observation.

To test our predictions, we compare to the optical conductivity spectrum of BiTeI measured by Lee and co-workers [70], and shown in Fig. 5. It is important to note that experimental samples are typically n doped, and the data shown in Fig. 5 corresponds to two different samples with doping concentrations of $n = 0.4 \times 10^{19}$ cm^{-3} with the Fermi level near the bottom of the conduction band (left diagram), and of $n = 4.0 \times 10^{19}$ cm^{-3} with the Fermi level near the
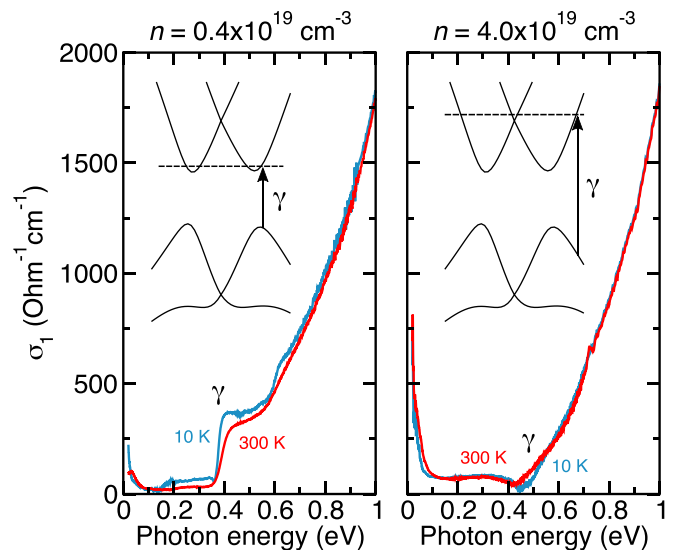

FIG. 5. Experimental optical conductivity σ_1 of BiTeI at an electron doping concentration of $n = 0.4 \times 10^{19}$ cm^{-3} (left) and $n = 4.0 \times 10^{19}$ cm^{-3} (right) at 10 K (blue curves) and at 300 K (red curves). The inset diagrams depict the position of the Fermi level (dashed line) within the Rashba-split conduction bands, and the relevant interband γ transition. The experimental data was provided by Lee and is partially published in Ref. [70].

crossing of the Rashba-split bands (right diagram) [70]. In both cases we focus on the band gap determined by the interband γ transition, which is indicated in the insets of Fig. 5, although we note that intraband transitions between the spin-split conduction bands are also observed [70,71]. For the weakly doped sample, the size of the band gap increases with increasing temperature (the position of the γ edge shifts to higher energies). This is consistent with our prediction of the increase of the band gap with increasing temperature for BiTeI. In the more highly doped sample, the position of the γ edge exhibits the opposite behavior, and shifts to lower energies with increasing temperature. In this latter sample, the Fermi level sits around the crossing point between the spin-split bands. Assuming that the only effects of doping are a rigid shift of the Fermi level, then our results for BiTeI also agree with this observation. This is because, as shown in Fig. 2, for electronic states of wave vectors at distances larger than about 80×10^{-3} Å^{-1} from the A point, the energy gap decreases with increasing temperature. This comparison confirms our predictions, and highlights the complex interplay between the level of doping and the temperature dependence of the band structure as measured by optical probes. We note that the temperature dependence of the band gap of BiTeBr and BiTeCl is reported in Refs. [72,73], where a decrease of the band gap with increasing temperature is observed in samples with a significant level of electron doping. The results in Fig. 2 for BiTeCl are consistent with this scenario for sufficient electron doping. In contrast, for BiTeBr there is no level of electron doping that would lead to a band gap decrease with increasing temperature, and therefore our calculations are not consistent with the reported measurements on this material. A possible origin for this discrepancy could be a renormalization of the bands when electron doped.

An alternative experimental test of our predictions would be to use angle-resolved photoemission spectroscopy (ARPES), which could provide a direct measurement of the temperature-induced changes to the Rashba-split bands. However, using this technique it might be difficult to disentangle the bulk and surface dispersions [13–15]. In this context, another consequence of our results is to question the use of standard first-principles calculations to interpret ARPES experiments in this class of materials. The original report of giant Rashba splitting in BiTeI was based on ARPES measurements [13]. One of the arguments in support of the bulk nature of this Rashba splitting was the good agreement of the experimental Rashba parameters with first-principles calculations based on a generalized gradient approximation (GGA) to the exchange-correlation functional and performed at zero temperature. Subsequent experiments questioned the bulk nature of the Rashba splitting reported in Ref. [13], as ultraviolet ARPES probing the surface bands led to a dispersion in good agreement with that of Ref. [13], but soft x-ray ARPES probing the bulk bands showed that the surface Rashba parameter was 20% larger than the bulk parameter [15]. Again, part of the justification for these results was the support of first-principles GGA calculations. Our results show the changes in the Rashba parameters induced by temperature are comparable to the measured difference between surface and bulk Rashba splittings. Together with previously reported contributions from electron correlation [25], which are similar in size to those from temperature effects, our results show that predictions using first-principles semilocal DFT methods within the static lattice approximation have to be interpreted with caution.

More generally, our work contributes to the investigations of the interplay between temperature and spin-orbit physics. Giant Rashba splittings have been reported in the hybrid halide perovskites [74], and it has been argued that this effect is enhanced by the temperature-induced molecular rotations of the dipolar cation [75]. Recent studies have reported significant effects of temperature on the properties of topological insulators and Weyl semimetals, including temperature-induced topological phase transitions [51,67,76–80].

IV. SUMMARY

We have performed first-principles calculations to study the temperature dependence of the Rashba splitting in the bismuth tellurohalides. We find a reduction in the Rashba splitting with increasing temperature which is particularly strong in BiTeI, with a 40% change in going from 0 to 300 K. We find the opposite behavior when BiTeI has inverted bands in the topological-insulator phase, with temperature enhancing the Rashba splitting, and propose this reversal of the temperature dependency of the band gap as a signature for identifying a pressure-induced topological phase transition. Electron-phonon coupling and thermal expansion contribute similarly to the temperature dependence of the Rashba-split bands, and their microscopic behavior is dominated by the layered nature of the bismuth tellurohalide structures.

Overall, our results show that quantitative first-principles predictions of Rashba splitting must incorporate the effects of temperature. Furthermore, the temperature-induced changes that we predict in BiTeI are consistent with experimental optical conductivities, but we find a discrepancy between our results for BiTeBr and reported band gap temperature dependencies for this material. Additional measurements could provide further insights into the nature of Rashba splitting and topology in these materials.

[1] R. Winkler, *Spin-Orbit Coupling Effects in Two-Dimensional Electron and Hole Systems* (Springer, Berlin, 2003).

[2] M. Z. Hasan and C. L. Kane, *Colloquium*: Topological insulators, Rev. Mod. Phys. **82**, 3045 (2010).

[3] X.-L. Qi and S.-C. Zhang, Topological insulators and superconductors, Rev. Mod. Phys. **83**, 1057 (2011).

[4] Yu. A. Bychkov and E. I. Rashba, Properties of a 2D electron gas with lifted spectral degeneracy, Pis'ma Zh. Eksp. Teor. Fiz. **39**, 66 (1984) [JETP Lett. **39**, 78 (1984)].

[5] Yu. A. Bychkov and E. I. Rashba, Oscillatory effects and the magnetic susceptibility of carriers in inversion layers, J. Phys. C **17**, 6039 (1984).

[6] J. Sinova, D. Culcer, Q. Niu, N. A. Sinitsyn, T. Jungwirth, and A. H. MacDonald, Universal Intrinsic Spin Hall Effect, Phys. Rev. Lett. **92**, 126603 (2004).

[7] V. M. Edelstein, Spin polarization of conduction electrons induced by electric current in two-dimensional asymmetric electron systems, Solid State Commun. **73**, 233 (1990).

[8] S. D. Ganichev, E. L. Ivchenko, V. V. Bel'kov, S. A. Tarasenko, M. Sollinger, D. Weiss, W. Wegscheider, and W. Prettl, Spin-galvanic effect, Nature (London) **417**, 153 (2002).

[9] E. Bauer, G. Hilscher, H. Michor, Ch. Paul, E. W. Scheidt, A. Gribanov, Yu. Seropegin, H. Noël, M. Sigrist, and P. Rogl, Heavy Fermion Superconductivity and Magnetic Order in Noncentrosymmetric CePt$_3$Si, Phys. Rev. Lett. **92**, 027003 (2004).

[10] I. Žutić, J. Fabian, and S. Das Sarma, Spintronics: Fundamentals and applications, Rev. Mod. Phys. **76**, 323 (2004).

[11] C. R. Ast, J. Henk, A. Ernst, L. Moreschini, M. C. Falub, D. Pacilé, P. Bruno, K. Kern, and M. Grioni, Giant Spin Splitting Through Surface Alloying, Phys. Rev. Lett. **98**, 186807 (2007).

[12] J. Nitta, T. Akazaki, H. Takayanagi, and T. Enoki, Gate Control of Spin-Orbit Interaction in an Inverted In$_{0.53}$Ga$_{0.47}$As/I$_{0.52}$Al$_{0.48}$As Heterostructure, Phys. Rev. Lett. **78**, 1335 (1997).

[13] K. Ishizaka, M. S. Bahramy, H. Murakawa, M. Sakano, T. Shimojima, T. Sonobe, K. Koizumi, S. Shin, H. Miyahara,

A. Kimura, K. Miyamoto, T. Okuda, H. Namatame, M. Taniguchi, R. Arita, N. Nagaosa, K. Kobayashi, Y. Murakami, R. Kumai, Y. Kaneko, Y. Onose, and Y. Tokura, Giant Rashba-type spin splitting in bulk BiTeI, Nat. Mater. **10**, 521 (2011).

[14] A. Crepaldi, L. Moreschini, G. Autès, C. Tournier-Colletta, S. Moser, N. Virk, H. Berger, Ph. Bugnon, Y. J. Chang, K. Kern, A. Bostwick, E. Rotenberg, O. V. Yazyev, and M. Grioni, Giant Ambipolar Rashba Effect in the Semiconductor BiTeI, Phys. Rev. Lett. **109**, 096803 (2012).

[15] G. Landolt, S. V. Eremeev, Y. M. Koroteev, B. Slomski, S. Muff, T. Neupert, M. Kobayashi, V. N. Strocov, T. Schmitt, Z. S. Aliev, M. B. Babanly, I. R. Amiraslanov, E. V. Chulkov, J. Osterwalder, and J. H. Dil, Disentanglement of Surface and Bulk Rashba Spin Splittings in Noncentrosymmetric BiTeI, Phys. Rev. Lett. **109**, 116403 (2012).

[16] M. Sakano, M. S. Bahramy, A. Katayama, T. Shimojima, H. Murakawa, Y. Kaneko, W. Malaeb, S. Shin, K. Ono, H. Kumigashira, R. Arita, N. Nagaosa, H. Y. Hwang, Y. Tokura, and K. Ishizaka, Strongly Spin-Orbit Coupled Two-Dimensional Electron Gas Emerging Near the Surface of Polar Semiconductors, Phys. Rev. Lett. **110**, 107204 (2013).

[17] M. S. Bahramy and N. Ogawa, Bulk Rashba semiconductors and related quantum phenomena, Adv. Mater. **29**, 1605911 (2017).

[18] M. S. Bahramy, R. Arita, and N. Nagaosa, Origin of giant bulk Rashba splitting: Application to BiTeI, Phys. Rev. B **84**, 041202 (2011).

[19] S. V. Eremeev, I. A. Nechaev, Yu. M. Koroteev, P. M. Echenique, and E. V. Chulkov, Ideal Two-Dimensional Electron Systems with a Giant Rashba-type Spin Splitting in Real Materials: Surfaces of Bismuth Tellurohalides, Phys. Rev. Lett. **108**, 246802 (2012).

[20] D. Di Sante, P. Barone, R. Bertacco, and S. Picozzi, Electric control of the giant Rashba effect in bulk GeTe, Adv. Mater. **25**, 509 (2013).

[21] M. Kim, J. Im, A. J. Freeman, J. Ihm, and H. Jin, Switchable $S = 1/2$ and $J = 1/2$ Rashba bands in ferroelectric halide perovskites, Proc. Natl. Acad. Sci. U.S.A. **111**, 6900 (2014).

[22] A. Narayan, Class of Rashba ferroelectrics in hexagonal semiconductors, Phys. Rev. B **92**, 220101 (2015).

[23] M. Liebmann, C. Rinaldi, D. Di Sante, J. Kellner, C. Pauly, R. N. Wang, J. E. Boschker, A. Giussani, S. Bertoli, M. Cantoni, L. Baldrati, M. Asa, I. Vobornik, G. Panaccione, D. Marchenko, J. Sanchez-Barriga, O. Rader, R. Calarco, S. Picozzi, R. Bertacco, and M. Morgenstern, Giant Rashba-type spin splitting in ferroelectric GeTe(111), Adv. Mater. **28**, 560 (2016).

[24] S. Güler-Kılıç and Ç. Kılıç, Crystal and electronic structure of BiTeI, AuTeI, and PdTeI compounds: A dispersion-corrected density-functional study, Phys. Rev. B **91**, 245204 (2015).

[25] I. P. Rusinov, I. A. Nechaev, S. V. Eremeev, C. Friedrich, S. Blügel, and E. V. Chulkov, Many-body effects on the Rashba-type spin splitting in bulk bismuth tellurohalides, Phys. Rev. B **87**, 205103 (2013).

[26] G. Kresse and J. Hafner, *Ab initio* molecular dynamics for liquid metals, Phys. Rev. B **47**, 558 (1993).

[27] G. Kresse and J. Hafner, *Ab initio* molecular-dynamics simulation of the liquid-metal-amorphous-semiconductor transition in germanium, Phys. Rev. B **49**, 14251 (1994).

[28] G. Kresse and J. Furthmüller, Efficiency of ab-initio total energy calculations for metals and semiconductors using a plane-wave basis set, Comput. Mater. Sci. **6**, 15 (1996).

[29] G. Kresse and J. Furthmüller, Efficient iterative schemes for *ab initio* total-energy calculations using a plane-wave basis set, Phys. Rev. B **54**, 11169 (1996).

[30] P. E. Blöchl, Projector augmented-wave method, Phys. Rev. B **50**, 17953 (1994).

[31] G. Kresse and D. Joubert, From ultrasoft pseudopotentials to the projector augmented-wave method, Phys. Rev. B **59**, 1758 (1999).

[32] D. D. Koelling and B. N. Harmon, A technique for relativistic spin-polarised calculations, J. Phys. C **10**, 3107 (1977).

[33] A. V. Shevelkov, E. V. Dikarev, R. V. Shpanchenko, and B. A. Popovkin, Crystal structures of bismuth tellurohalides BiTe*X* ($X = $ Cl, Br, I) from x-ray powder diffraction data, J. Solid State Chem. **114**, 379 (1995).

[34] D. M. Ceperley and B. J. Alder, Ground State of the Electron Gas by a Stochastic Method, Phys. Rev. Lett. **45**, 566 (1980).

[35] J. P. Perdew and A. Zunger, Self-interaction correction to density-functional approximations for many-electron systems, Phys. Rev. B **23**, 5048 (1981).

[36] J. P. Perdew and Y. Wang, Accurate and simple analytic representation of the electron-gas correlation energy, Phys. Rev. B **45**, 13244 (1992).

[37] J. P. Perdew, K. Burke, and M. Ernzerhof, Generalized Gradient Approximation Made Simple, Phys. Rev. Lett. **77**, 3865 (1996).

[38] J. P. Perdew, A. Ruzsinszky, G. I. Csonka, O. A. Vydrov, G. E. Scuseria, L. A. Constantin, X. Zhou, and K. Burke, Restoring the Density-Gradient Expansion for Exchange in Solids and Surfaces, Phys. Rev. Lett. **100**, 136406 (2008).

[39] A. Tkatchenko and M. Scheffler, Accurate Molecular van der Waals Interactions from Ground-State Electron Density and Free-Atom Reference Data, Phys. Rev. Lett. **102**, 073005 (2009).

[40] S. Güler-Kılıç and Ç. Kılıç, Pressure dependence of the band-gap energy in BiTeI, Phys. Rev. B **94**, 165203 (2016).

[41] K. Kunc and R. M. Martin, *Ab Initio* Force Constants of GaAs: A New Approach to Calculation of Phonons and Dielectric Properties, Phys. Rev. Lett. **48**, 406 (1982).

[42] J. H. Lloyd-Williams and B. Monserrat, Lattice dynamics and electron-phonon coupling calculations using nondiagonal supercells, Phys. Rev. B **92**, 184301 (2015).

[43] I. Yu. Sklyadneva, R. Heid, K.-P. Bohnen, V. Chis, V. A. Volodin, K. A. Kokh, O. E. Tereshchenko, P. M. Echenique, and E. V. Chulkov, Lattice dynamics of bismuth tellurohalides, Phys. Rev. B **86**, 094302 (2012).

[44] P. B. Allen and V. Heine, Theory of the temperature dependence of electronic band structures, J. Phys. C **9**, 2305 (1976).

[45] F. Giustino, S. G. Louie, and M. L. Cohen, Electron-Phonon Renormalization of the Direct Band Gap of Diamond, Phys. Rev. Lett. **105**, 265501 (2010).

[46] B. Monserrat and R. J. Needs, Comparing electron-phonon coupling strength in diamond, silicon, and silicon carbide: First-principles study, Phys. Rev. B **89**, 214304 (2014).

[47] S. Poncé, Y. Gillet, J. Laflamme Janssen, A. Marini, M. Verstraete, and X. Gonze, Temperature dependence of the electronic structure of semiconductors and insulators, J. Chem. Phys. **143**, 102813 (2015).

[48] C. E. Patrick and F. Giustino, Quantum nuclear dynamics in the photophysics of diamondoids, Nat. Commun. **4**, 2006 (2013).

[49] B. Monserrat, Vibrational averages along thermal lines, Phys. Rev. B **93**, 014302 (2016).

[50] M. T. Dove, *Introduction to Lattice Dynamics* (Cambridge University Press, Cambridge, 1993).

[51] K. Saha and I. Garate, Phonon-induced topological insulation, Phys. Rev. B **89**, 205103 (2014).

[52] M. S. Bahramy, B. J. Yang, R. Arita, and N. Nagaosa, Emergence of non-centrosymmetric topological insulating phase in BiTeI under pressure, Nat. Commun. **3**, 679 (2012).

[53] S. Murakami and S.-i. Kuga, Universal phase diagrams for the quantum spin Hall systems, Phys. Rev. B **78**, 165313 (2008).

[54] J. Liu and D. Vanderbilt, Weyl semimetals from noncentrosymmetric topological insulators, Phys. Rev. B **90**, 155316 (2014).

[55] X. Xi, C. Ma, Z. Liu, Z. Chen, W. Ku, H. Berger, C. Martin, D. B. Tanner, and G. L. Carr, Signatures of a Pressure-Induced Topological Quantum Phase Transition in BiTeI, Phys. Rev. Lett. **111**, 155701 (2013).

[56] Y. Chen, X. Xi, W.-L. Yim, F. Peng, Y. Wang, H. Wang, Y. Ma, G. Liu, C. Sun, C. Ma, Z. Chen, and H. Berger, High-pressure phase transitions and structures of topological insulator BiTeI, J. Phys. Chem. C **117**, 25677 (2013).

[57] T. Ideue, J. G. Checkelsky, M. S. Bahramy, H. Murakawa, Y. Kaneko, N. Nagaosa, and Y. Tokura, Pressure variation of Rashba spin splitting toward topological transition in the polar semiconductor BiTeI, Phys. Rev. B **90**, 161107 (2014).

[58] J. Park, K.-H. Jin, Y. J. Jo, E. S. Choi, W. Kang, E. Kampert, J.-S. Rhyee, S.-H. Jhi, and J. S. Kim, Quantum oscillation signatures of pressure-induced topological phase transition in BiTeI, Sci. Rep. **5**, 15973 (2015).

[59] Y. Qi, W. Shi, P. G. Naumov, N. Kumar, R. Sankar, W. Schnelle, C. Shekhar, F.-C. Chou, C. Felser, B. Yan, and S. A. Medvedev, Topological quantum phase transition and superconductivity induced by pressure in the bismuth tellurohalide BiTeI, Adv. Mater. **29**, 1605965 (2017).

[60] M. K. Tran, J. Levallois, P. Lerch, J. Teyssier, A. B. Kuzmenko, G. Autès, O. V. Yazyev, A. Ubaldini, E. Giannini, D. van der Marel, and A. Akrap, Infrared- and Raman-Spectroscopy Measurements of a Transition in the Crystal Structure and a Closing of the Energy Gap of BiTeI under Pressure, Phys. Rev. Lett. **112**, 047402 (2014).

[61] Y. L. Chen, M. Kanou, Z. K. Liu, H. J. Zhang, J. A. Sobota, D. Leuenberger, S. K. Mo, B. Zhou, S-L. Yang, P. S. Kirchmann, D. H. Lu, R. G. Moore, Z. Hussain, Z. X. Shen, X. L. Qi, and T. Sasagawa, Discovery of a single topological Dirac fermion in the strong inversion asymmetric compound BiTeCl, Nat. Phys. **9**, 704 (2013).

[62] I. P. Rusinov, T. V. Menshchikova, I. Yu Sklyadneva, R. Heid, K.-P. Bohnen, and E. V. Chulkov, Pressure effects on crystal and electronic structure of bismuth tellurohalides, New J. Phys. **18**, 113003 (2016).

[63] I. Crassee, F. Borondics, M. K. Tran, G. Autès, A. Magrez, P. Bugnon, H. Berger, J. Teyssier, O. V. Yazyev, M. Orlita, and A. Akrap, BiTeCl and BiTeBr: A comparative high-pressure optical study, Phys. Rev. B **95**, 045201 (2017).

[64] A. Ohmura, Y. Higuchi, T. Ochiai, M. Kanou, F. Ishikawa, S. Nakano, A. Nakayama, Y. Yamada, and T. Sasagawa, Pressure-induced topological phase transition in the polar semiconductor BiTeBr, Phys. Rev. B **95**, 125203 (2017).

[65] D. Gresch, G. Autès, O. V. Yazyev, M. Troyer, D. Vanderbilt, B. A. Bernevig, and A. A. Soluyanov, Z2Pack: Numerical implementation of hybrid Wannier centers for identifying topological materials, Phys. Rev. B **95**, 075146 (2017).

[66] A. A. Soluyanov and D. Vanderbilt, Computing topological invariants without inversion symmetry, Phys. Rev. B **83**, 235401 (2011).

[67] B. Monserrat and D. Vanderbilt, Temperature Effects in the Band Structure of Topological Insulators, Phys. Rev. Lett. **117**, 226801 (2016).

[68] G. Antonius, S. Poncé, P. Boulanger, M. Côté, and X. Gonze, Many-Body Effects on the Zero-Point Renormalization of the Band Structure, Phys. Rev. Lett. **112**, 215501 (2014).

[69] B. Monserrat, Correlation effects on electron-phonon coupling in semiconductors: Many-body theory along thermal lines, Phys. Rev. B **93**, 100301 (2016).

[70] J. S. Lee, G. A. H. Schober, M. S. Bahramy, H. Murakawa, Y. Onose, R. Arita, N. Nagaosa, and Y. Tokura, Optical Response of Relativistic Electrons in the Polar BiTeI Semiconductor, Phys. Rev. Lett. **107**, 117401 (2011).

[71] C. Martin, K. H. Miller, S. Buvaev, H. Berger, X. S. Xu, A. F. Hebard, and D. B. Tanner, Temperature dependent infrared spectroscopy of the Rashba spin-splitting semiconductor BiTeI, arXiv:1209.1656.

[72] A. Akrap, J. Teyssier, A. Magrez, P. Bugnon, H. Berger, A. B. Kuzmenko, and D. van der Marel, Optical properties of BiTeBr and BiTeCl, Phys. Rev. B **90**, 035201 (2014).

[73] C. Martin, A. V. Suslov, S. Buvaev, A. F. Hebard, P. Bugnon, H. Berger, A. Magrez, and D. B. Tanner, Unusual Shubnikov–de Haas oscillations in BiTeCl, Phys. Rev. B **90**, 201204 (2014).

[74] D. Niesner, M. Wilhelm, I. Levchuk, A. Osvet, S. Shrestha, M. Batentschuk, C. Brabec, and T. Fauster, Giant Rashba Splitting in $CH_3NH_3PbBr_3$ Organic-Inorganic Perovskite, Phys. Rev. Lett. **117**, 126401 (2016).

[75] P. Azarhoosh, S. McKechnie, J. M. Frost, A. Walsh, and M. van Schilfgaarde, Relativistic origin of slow electron-hole recombination in hybrid halide perovskite solar cells, APL Mater. **4**, 091501 (2016).

[76] I. Garate, Phonon-Induced Topological Transitions and Crossovers in Dirac Materials, Phys. Rev. Lett. **110**, 046402 (2013).

[77] J. Kim and S.-H. Jhi, Topological phase transitions in group IV-VI semiconductors by phonons, Phys. Rev. B **92**, 125142 (2015).

[78] K. Saha, K. Légaré, and I. Garate, Detecting Band Inversions by Measuring the Environment: Fingerprints of Electronic Band Topology in Bulk Phonon Linewidths, Phys. Rev. Lett. **115**, 176405 (2015).

[79] G. Antonius and S. G. Louie, Temperature-Induced Topological Phase Transitions: Promoted Versus Suppressed Nontrivial Topology, Phys. Rev. Lett. **117**, 246401 (2016).

[80] L.-L. Wang, N. H. Jo, Y. Wu, Q. S. Wu, A. Kaminski, P. C. Canfield, and D. D. Johnson, Phonon-induced topological transition to a type-II Weyl semimetal, Phys. Rev. B **95**, 165114 (2017).